Final Report
on

Evaluation of Synthetic Aperture Radar (SAR) Image Compression Techniques

Güner Arslan and Magesh Valliappan

EE381K
Multidimensional Signal Processing
Prof. Brian L. Evans

December 6, 1998

Abstract

With the improvement of synthetic aperture radar (SAR) technology, larger areas are being imaged and the resolution of the images has increased. Larger images have to be transmitted and stored. Due to the limited storage and/or downlink capacity on the airplane or satellite, the volume of the data must be reduced. This makes compression of SAR images with minimal loss of information important. Mean squared error (MSE) and peak signal-to-noise ratio (PSNR) are the commonly quoted performance measures for comparing the compression algorithms. However, these measures inherently assume that the distortion is image independent noise, which is not a valid assumption in image compression algorithms. We propose a way to measure the distortion caused by compression and decompression of an image, by decoupling the distortion into a linear effect and additive uncorrelated noise, which models the nonlinear distortion. Using this procedure, the linear frequency distortion can be quantified by a weighted mean of the deviation from an all-pass system. The noise can be weighted according to a specific application before measuring the signal to noise ratio. Since the nonlinear distortion, such as blocking effect and mosquito noise, is a high frequency effect, we use a discrete Laplacian operator to emphasize higher frequencies in the image and use a measure correlation measure to quantify this distortion. Our simulation results show that the proposed metrics are consistent with image quality.

1 Introduction

Synthetic Aperture Radar (SAR) is an active remote sensing system which has applications in agriculture, ecology, geology, oceanography, hydrology and in the military [1]. SAR systems increase their effective aperture by using the motion of a satellite or an airplane they are mounted on. The primary reason which gives SAR systems such diverse applications is that they have the ability to take images in all weather conditions.

With the improvement of SAR technology, larger areas are being imaged and the resolution of the images has increased. This causes larger images to be transmitted and stored. Due to the limited storage and/or downlink capacity on the airplane or satellite the data rate must be reduced. This motivates the compression of SAR images. The high entropy of SAR images results in very low compression ratios when lossless compression techniques are used [1]. To achieve higher compression ratios, lossy image compression techniques are used [2, 3].

SAR data is inherently complex-valued but it is frequently converted to real data for interpretation by human observers or machine algorithms [3]. However, when precise measurement of topographic elevation is required (interferometric SAR), the phase information is very important. Thus to preserve this information accurately, lossless or near lossless compression is required [4].

SAR imaging techniques introduce speckle noise, which is a form of multiplicative noise [5]. The presence of speckle noise and the fact that more useful information is contained in the higher frequency bands make SAR images quite different from optical images [6]. Due to these differences, classical image compression techniques do not perform as well when applied to SAR images [7, 8]. Although many different compression techniques have been applied to SAR images, they have been compared using peak signal-to-noise ratio or mean squared error [2, 7, 9, 10]. However, these measures inherently assume that the distortion is image independent noise, which is not a valid assumption in image compression algorithms. In this work, we propose three new quality metrics, which aim to quantify the linear and nonlinear distortions independently.

Section 2 briefly introduces the two compression techniques which we use in this work. Section 3 discusses the standard metrics and the metrics we propose. Sections 4 and 5 explain how we actually measure the distortion and discussed the results we obtain. Section 6 concludes the work.

2 Lossy Image Compression Techniques

In this work, we choose two lossy image compression techniques and apply them to SAR images. One of these, the Joint Photographic Experts Group (JPEG) algorithm, is the presently

accepted lossy still image compression standard. JPEG is a discrete cosine transform (DCT) based image compression standard. The primary advantage of JPEG is its low computational complexity and the availability of fast hardware and software implementations. At high compression ratios the quality of JPEG compressed images degrade due to severe blocking artifacts.

The other algorithm, set partitioning in hierarchical trees (SPIHT), is a more recent, discrete wavelet transform (DWT) based compression technique [11]. DWT based techniques, in general, give compressed images of better visual quality. However, at very high compression ratios, artifacts in the form of mosquito noise become visible.

3 Quality Metrics

Since the aim of image compression is to reduce the number of bits required to represent a image without destroying useful information, a measure of image quality for a fixed compression ratio is required.

3.1 Commonly used Quality Measures

The mean squared error (MSE) is one of the commonly used performance measures in image and signal processing. For an image of size $N \times M$ it can be defined as

$$\text{MSE} = \frac{1}{NM} \sum_{n=0}^{N-1} \sum_{m=0}^{M-1} (x[n,m] - \hat{x}[n,m])^2$$

where $x[n,m]$ is the original image and $\hat{x}[n,m]$ is the decompressed image. Peak signal-to-noise ratio (PSNR) is a variation of MSE and is defined as,

$$\text{PSNR} = 10 \log_{10} \frac{(\text{ peak-to-peak value of the original image })^2}{\text{MSE}}$$

These metrics assume that the distortion is caused only by additive, image independent noise. Since the difference between the decompressed and the original image is not uncorrelated noise, this assumption is invalid. However, they are commonly used in image processing applications due to the lack of a more appropriate simple metric.

3.2 Alternative Quality Measures

The overall degradation of an image can usually be decoupled into two effects - *frequency distortion* and *noise injection*. These two effects are different in nature and have to be quantified separately. The compression - decompression scheme has to be modeled as a linear filtering operation followed by the addition of an uncorrelated noise image as shown in Figure 1. We can

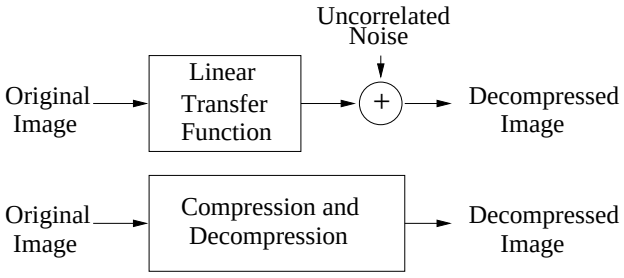

Figure 1: Model of compression-decompression

define a distortion transfer function (DTF) as the deviation of the linear model from an all-pass system. Since the noise image is now uncorrelated, it can be used with an appropriate noise measure. Based on the application of the SAR images we can weight the DTF and the noise image in the frequency domain to obtain application-specific metrics, weighted signal-to-noise ratio (WSNR) and a linear distortion measure. In this work, we consider SAR images that are interpreted by humans and therefore use a linear model of the human visual system to derive suitable weighting functions [13].

The noise image is uncorrelated with the original image, but not independent. As a result, nonlinear distortions are also treated as uncorrelated noise. However, the magnitude of the nonlinear distortions, such as blocking artifacts and mosquito noise, is significant only at high compression ratios. These artifacts are predominantly high frequency effects. So, filtering the decompressed images to extract the edge information enhances the effect of these artifacts. A measure of the correlation between this image and a similarly filtered version of the original image can be used to give a metric for nonlinear distortion. SAR images have useful edge and texture information, which are also emphasized by this technique.

4 Implementation of the Metrics

The images we use in our simulations were acquired by the Spaceborne Imaging Radar-C/X-Synthetic Aperture Radar (SIR-C/X-SAR) [12]. Since the original images are too large to handle we crop them to 512×512 8 bit grayscale sub-images. The simulations are performed on several images representing different geographical regions such as cities, rivers, volcanos and oceans. Since the distortion becomes severe we do not go beyond compression ratios of 8:1.

4.1 Pre-filtering

The nature of SAR imaging systems causes SAR images to be corrupted by speckle noise. Speckle noise removal is a research area by itself and is not a part of this work. However,

since speckle noise affects the compression ratio of an image, we pre-filter our images with a 3×3 σ-filter, which has been used in the literature for speckle noise removal [5]. The σ-filter is a selective averaging filter, which excludes those pixels within the window that are beyond a range ($\pm\sigma$) of the center pixel. σ has to be chosen suitably to obtain sufficient noise smoothing and at the same time preserve edges.

The σ-filter however is not capable of handling spot noise. When all the surrounding pixels lie outside the range ($\pm\sigma$) the σ-filter does not perform any averaging. We modify the σ-filter to handle this special case, by replacing the pixel by the average of all the other pixels within the window. The results are shown in Figure 2. The difference image shows the pixels where the modification of the filter has had an effect.

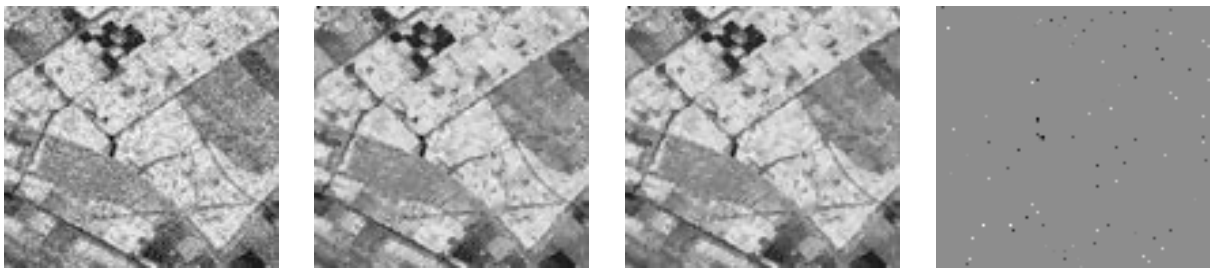

(a) (b) (c) (d)

Figure 2: (a) Original image (b) Original σ filter (c) Modified σ filter (d) difference of (b) and (c)

4.2 Estimation of the Linear Model and Noise Image

Starting with the 512×512 original image we form a 1024×1024 image by reflecting the image in both dimensions. We similarly form a 1024×1024 image from the decompressed image. This helps to reduce the effect of false edges across image borders in the discrete Fourier transform (DFT). We model the linear filtering operation as a wraparound convolution of the extended original image and a linear filter. We also assume that the filters have a small region of support. This assumption is valid for the JPEG and SPIHT algorithms since JPEG uses 8×8 block processing and SPIHT uses 9/7 tap filters. Therefore, we can assume that the filter's frequency response is slowly varying in frequency domain.

We compute the DFTs of the extended original and decompressed images. Then, we divide the frequency domain into 256 non-overlapping windows each of size 64×64. We assume that the transfer function is constant in each window and then estimate its value for each window independently. For each window we rearrange the encompassed elements of the DFT of the images to form column vectors, denoted by $\mathbf{x}$ and $\mathbf{y}$ for the original and decompressed, respectively. We compute H, the frequency response of the model in each window, such that

$\mathbf{e} = \mathbf{y} - H\mathbf{x}$ is uncorrelated with $\mathbf{x}$. That is

$$\mathbf{e}^H\mathbf{x} = (\mathbf{y} - H\mathbf{x})\mathbf{x} = 0 \text{ thus } H = (\mathbf{y}^H\mathbf{x})/(\mathbf{x}^H\mathbf{x})$$

It can be shown that this is the optimal solution for H also in the least squares sense.

Having estimated H in each window, we now have an estimate of a linear model. To estimate the noise image we have to extract the linear component from the original image. This filtering operation is done in frequency domain and after the inverse DFT we obtain a 1024×1024 filtered image. The noise image is obtained by extracting the 512×512 sub-image from the difference of the extended original image and the filtered image.

4.3 Computation of the Weighted Signal-to-Noise Ratio

Since SAR images are also interpreted by humans, an important performance measure is the visual quality of the decompressed image. Although the human visual system is a nonlinear, shift-varying, non-separable, non-uniformly sampled system, linear models have been proposed to approximate it [13][14]. The contrast sensitivity function (CSF), under the assumption of a linear model, determines the visibility of individual Fourier components of an image, as seen by a human observer. Using the CSF as a weighting function we obtain

$$\text{WSNR} \quad = 10 \log_{10} \left(\frac{\sum_u \sum_v |X(u,v)C(u,v)|^2}{\sum_u \sum_v |(D(u,v))C(u,v)|^2} \right)$$

where $X(u,v) and D(u,v)$ are the discrete Fourier transforms of the original image, noise image respectively and $C(u,v)$ is the CSF (Figure 3 (d)) [13][14].

4.4 Computation of Linear Distortion Measure

We can measure the distortion introduced by a linear transfer function by measuring the deviation from an all-pass transfer function. We define $1 - H(\omega_1, \omega_2)$ as the DTF corresponding to the transfer function $H(\omega_1, \omega_2)$. The DTF is weighted by the CSF to obtain a measure of linear distortion, as perceived by a human observer.

4.5 Correlation of Edge Information

To extract the edge information we use a 3×3 discrete approximation of a Laplacian operator. To measure the correlation between the filtered original image and the filtered decompressed image we compute the magnitude of the correlation coefficient, which is given by

$$C_{XY} = \frac{|\text{Covariance}(X,Y)|}{\sigma_X \sigma_Y} \tag{1}$$

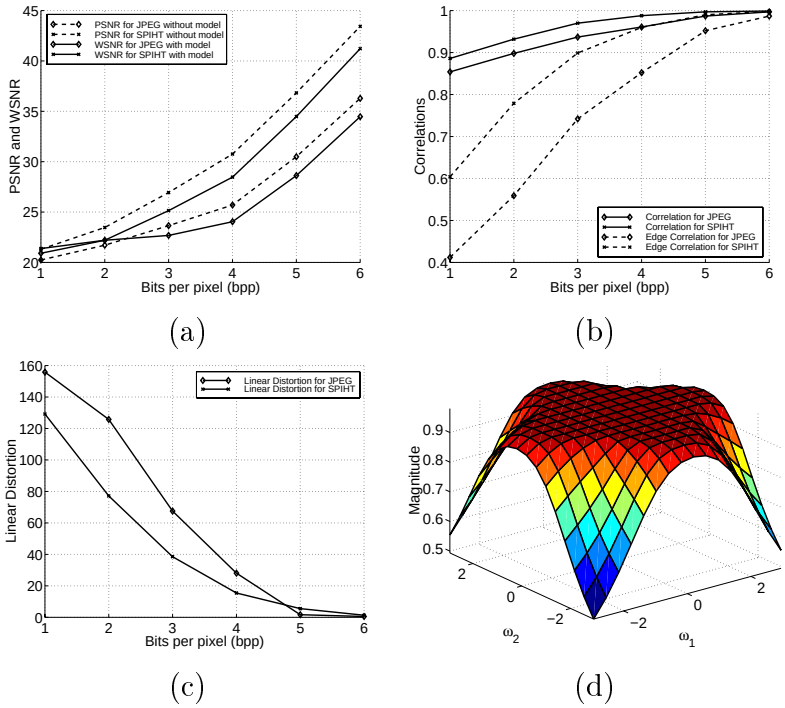

Figure 3: Proposed metrics and PSNR versus compression ratio (a) PSNR and WSNR values for JPEG and SPIHT with and without using the proposed model (b) Original and decompressed image correlation (c) Linear distortion measure (d) Contrast Sensitivity Function

5 Results

The results obtained for a SAR image of the city of Houston are presented here. The results obtained from WSNR/PSNR are shown in Figure 3 (a). PSNR shows that SPIHT outperforms JPEG consistently at all compression ratios. However, WSNR results are closer and in fact at lower compression ratios (2 bits per pixel) the noise performance is comparable and this is verified by visual inspection of the images. This is because SPIHT generates more low frequency noise and hence the visual effect of the noise is comparable to that of JPEG, even though the MSE is lower.

The frequency domain representations of the linear models of the compression schemes for this image at a compression ratio of 1.80 bits per pixel are shown in Figure 4. The linear models of both compression schemes are lowpass in nature. The JPEG algorithm almost completely filters out higher frequency components. The linear model of the SPIHT algorithm shows three levels corresponding to the subband decomposition technique with lower frequency bands being quantized to fewer bits. From the models it can be estimated that SPIHT linearly distorts the images lesser. The Linear Distortion Measure shows similar results for compression ratios in the range of 1-4 bits per pixel, as seen in Figure 3 (b).

The correlation between the decompressed image and the original image is close to 1 for both

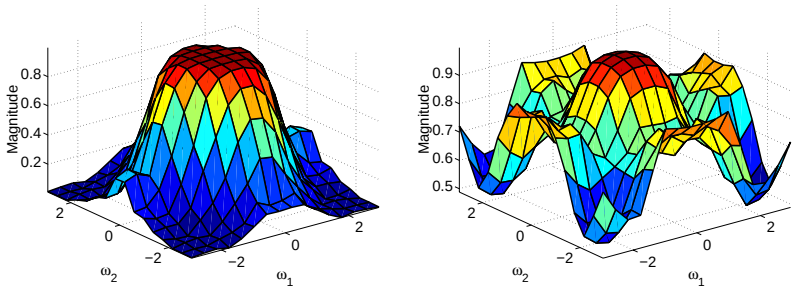

(a) (b)

Figure 4: (a) Linear Model for JPEG (b) Linear Model for SPIHT

compression techniques, with SPIHT doing better than JPEG (Figure 3 (c)). The correlation of edge information, however, shows that SPIHT does much better than JPEG, which is more consistent with the degree of nonlinear distortion observed in the images.

6 Conclusions

Although they are commonly used, standard performance measures such as MSE and PSNR are not appropriate measures for SAR image compression algorithms. This follows from the fact that these metrics are noise measures and assume signal independent noise which is not a valid assumption in image compression algorithms. In this work we propose a new framework for evaluating the distortion introduced by compression. We measure the linear distortion by modeling the compression-decompression procedure as a linear filtering operation followed by the addition of uncorrelated noise. Both the linear distortion measure and the noise quality measure can be weighted in frequency domain depending on the application. We use the contrast sensitivity function, which is based on a linear model of the human visual system, to weight these measures assuming the decompressed images are consumed by humans. With high compression ratios, however, the additive noise approximation is invalid and the noise measures are inappropriate. In this case we use the correlation of edge information, which gives us a better measure of the nonlinear distortion, since the distortion is primarily a high frequency effect. We have tested the metrics on several SAR images and conclude that these metrics give more consistent results compared to the commonly applied metrics.

References

[1] R. W. Ives, *On the Compression of Synthetic Aperture Radar Imagery.* PhD thesis, Dept. of Electrical and Computer Engineering, The University of New Mexico, Albuquerque, New Mexico, May 1998.

[2] F. Sakarya and S. Emek, "SAR image compression," in *Proc. Asilomar Conf. Signals, Systems, and Comp.*, vol. 2, pp. 858–862, Nov. 1996.

[3] A. S. Werness, C. Susan, C. Wei, and R. Carpinella, "Experiments with wavelets for compression of SAR data," *IEEE Trans. Geoscience and Remote Sensing*, vol. 32, pp. 197–201, Jan. 1994.

[4] M. Brandfass, W. Coester, U. Benz, and A. Moreira, "Wavelet based approaches for efficient compression of complex sar image data," in *Int. Geoscience and Remote Sensing Symposium*, vol. 4, (Singapure, Singapure), pp. 2024–2027, Aug. 1997.

[5] D. Wei, J. Odegard, H. Gue, M. Land, and C. Burrus, "Simultaneous noise reduction and SAR image data compression using best wavelet packet basis," in *Proc. IEEE Int. Conf. Image Proc.*, vol. 3, (Washington, D.C.), pp. 200–203, Oct. 1995.

[6] M. Dutkiewicz and I. Cumming, "Evaluation of the effect of encoding on SAR data," *Photogrammetric Engineering and Remote Sensing*, vol. 60, pp. 895–904, Jul. 1994.

[7] M. Datcu, G. Schwarz, K. Schmidt, and C. Reck, "Quality evaluation of compressed optical and SAR images: JPEG vs. wavelets," in *Int. Geoscience and Remote Sensing Symposium*, vol. 3, (Richmond, BC, Canada), pp. 1678–1689, Jul. 1995.

[8] G. Staples, S. Rossignol, W. Stevens, and T. Stein, "Data compression effects on SAR image compression," in *Int. Geoscience and Remote Sensing Symposium*, vol. 3, (Richmond, BC, Canada), pp. 1678–1680, Jul. 1995.

[9] U. Benz, K. Strodl, and A. Moriera, "Comparison of several algorithms for SAR raw data compression," *IEEE Trans. Geoscience and Remote Sensing*, vol. 33, pp. 1266–1276, Sep. 1995.

[10] F. Sakarya and S. Emek, "An evaluation of SAR image compression techniques," in *Int. Conf. on Acoustics, Speech and Signal Proc. (ICASSP)*, vol. 4, pp. 2833–2836, Apr. 1997.

[11] A. Said and W. A. Pearlman, "A new fast and efficient image codec based on set partitioning in hierarchical trees," *IEEE Trans. Circuits and Systems for Video Technology*, vol. 6, pp. 243–250, Jun. 1996.

[12] JPL Imaging Radar web site at http://southport.jpl.nasa.gov/.

[13] T. Kite, *Design and Quality Assesment of Forward and Inverse Error Diffusion Halftoning Algortihms*. PhD thesis, The University of Texas at Austin, Austin, Texas, Aug. 1998.

[14] N. Damera-Venkata, T. Kite, B. Geisler, B. L. Evans, and A. Bovik, "Quality assessment of inverse halftones." Submitted to the IEEE Trans. on Image Proc.